1997

A Probabilistic View of Problems in Form Error Estimation

Tai-Hung Yang
Iowa State University

John K. Jackman
Iowa State University, jkj@iastate.edu

A Probabilistic View of Problems in Form Error Estimation

Abstract
Form error estimation techniques based on discrete point measurements can lead to significant errors in form tolerance evaluation. By modeling surface profiles as random variables, we show how sample size and fitting techniques affect form error estimation. Depending on the surface characteristics, typical sampling techniques can result in estimation errors of as much as 50 percent. Another issue raised in the fitting approach is the metric p selection for the fitting objective. We show that for $p = 2$ and $p = \infty$, the selection does not appear to significantly affect the estimation of form errors

Keywords
curve fitting, error analysis, estimation, fits and tolerances, inspection, fitting techniques, probabilistic estimation, object recognition

Disciplines
Industrial Engineering | Systems Engineering

Comments
This is an article from *Journal of Manufacturing Science and Engineering, Transactions of the ASME* 119 (1997): 375, doi: 10.1115/1.2831116. Posted with permission.

Tai-Hung Yang

J. Jackman

Department of Industrial
and Manufacturing System Engineering,
Iowa State University
Ames, IA

A Probabilistic View of Problems in Form Error Estimation

Form error estimation techniques based on discrete point measurements can lead to significant errors in form tolerance evaluation. By modeling surface profiles as random variables, we show how sample size and fitting techniques affect form error estimation. Depending on the surface characteristics, typical sampling techniques can result in estimation errors of as much as 50 percent. Another issue raised in the fitting approach is the metric p selection for the fitting objective. We show that for $p = 2$ and $p = \infty$, the selection does not appear to significantly affect the estimation of form errors.

1 Introduction

Inspection systems that provide metrology information on discrete points from the surface of an object must use some type of fitting procedure to obtain more meaningful dimensional and form information. In this context, we can examine the deviations of the surface being measured and neglect for the moment uncertainties introduced by the inspection system. Consider the idealized geometric boundary shown in Fig. 1 where the desired form feature is a straight line and the profile P is the actual profile of the workpiece. Form tolerances (ANSI/ASME Y14.5M, 1982) specify a zone bounded by two offset profiles of the nominal surface which must enclose P. We need only specify the offset value and no datum is needed, i.e., the tolerance zone floats in space.

For a discrete set of points, we want to determine if profile P lies within the specified tolerance zone (in this case straightness). We are faced with the problem of making inferences about the limits of the zone with incomplete information on P. The limits of P, l_u and l_l, are separated by a distance, W, which must be compared with the tolerance zone specification. In practice P and the limits (l_u and l_l) are unknown because it is infeasible to take an infinite number of points on P. We can easily extend the same problem to form tolerances other than straightness. Thus, the sampling strategy (location and number of points) and sample data analysis are critical issues in the context of inspection using discrete sample points.

Murthy and Abdin (1980) and Shunmugam (1986, 1987a, 1987b, 1990, 1991) have already demonstrated that estimates of W obtained from the least squares method do not agree with the definition of form errors.

The two main approaches to resolve this problem have been curve fitting and computational geometry. The curve fitting approach uses L_p-norm estimation, e.g., Caskey et al. (1991, 1992), Dhanish and Shunmugam (1991), and Hopp (1993). Using computational geometry, planar feature boundaries are determined from the convex hull and supporting lines, while circular features require application of Voronoi diagrams, e.g., Etesami and Qiao (1989), Traband et al. (1989) and Roy and Zhang (1992).

The goal of L_p-norm estimation is to find the fit parameters that minimize the L_p norm

$$L_p = \left[\frac{1}{n}\sum_i |r_i|^p\right]^{1/p} \tag{1}$$

where r_i is the ith residual and the sum is over n data points. The residuals discussed in this paper are the normal deviations to the fitted geometric features. Least-squares fitting corresponds to the case of $p = 2$. The limit of L_p as $p \to \infty$ is the largest magnitude residual, so the L_∞ problem is to minimize the maximum magnitude residual—i.e., to find the minimum zone fit (Hopp, 1993). Huang et al. (1993), Kanada and Suzuki (1993) as well as many others proposed various algorithms to calculate the width of this minimum zone. Caskey et al. (1992) also conclude that the "minimum zone is the same as minimax (L_∞)". In testing existing published methods, they found that the Anderson-Watson-Osborne algorithm was more efficient for minimum zone evaluations. Using this same algorithm as Caskey (1992), we can reduce the original nonlinear problem to a sequence of linear L_∞-norm problems, each of which is solved as a standard LP problem using the FORTRAN subroutine CHEB (Barrodale and Phillips, 1975)[1] followed by the inexact line search (Anderson and Osborne, 1977) to ensure convergence (Gonin and Money, 1989).

Hopp (1993) reports that the bias and sensitivity errors of the fit will vary with p. As p increases, the sensitivity of the fit to point measurement error increases, but the bias with respect to the fit prescribed by tolerance theory decreases. Therefore, it is very difficult to develop general guidelines for the proper choice of a fitting objective for a practical coordinate measuring system. Least-squares fitting is widely used and widely debated, with many claiming that extremal fitting is better because it "conforms" to tolerance theory. In fact, the best choice of a fitting objective is that which produces the smallest combined uncertainty in the result. How to make the best choice is not at all clear (Hopp, 1993).

In choosing a sampling strategy, we must consider the location and number of sample points needed to inspect a workpiece. A variety of sampling techniques such as uniform sampling, random sampling, stratified random sampling, Hammersley sampling (Caskey et al., 1992; Hocken et al., 1993; Woo et al., 1993) have been investigated. Hocken et al. (1993) point out that uniform sampling is the most practical technique for normal users since it is much easier to program a measuring machine to sample at equal intervals in angle or space than it is to use any other sampling techniques. Caskey et al. (1992) prefer stratified random sampling and argue that it is more robust to feature waviness based on their simulation results. Even with this method, their results gave poor performance in estimation of form errors. They found that a large number of samples is necessary to obtain a low variance of the estimated form error based on a particular surface. The relationship between feature waviness and the sampling methods is still unknown.

Contributed by the Manufacturing Engineering Division for publication in the JOURNAL OF MANUFACTURING SCIENCE AND ENGINEERING. Manuscript received July 1994; revised Dec. 1995. Associate Technical Editor: J. Sutherland.

[1] Note that Caskey et al. (1992) use Abdelmalek's algorithm to get the linear mini-max solution.

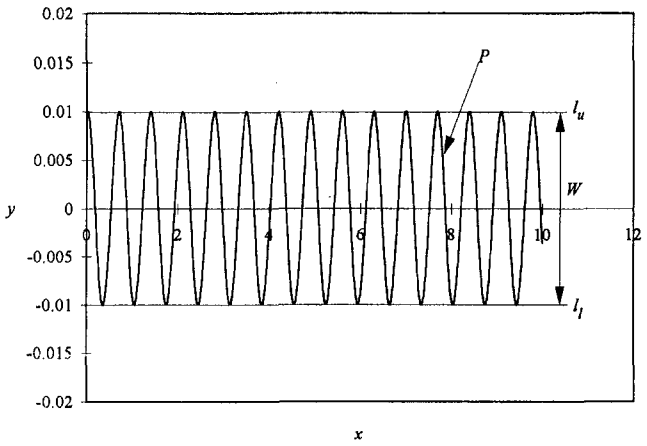

Fig. 1 Idealized geometric boundary ($y = .01 \cos(.1 - 9x)$)

We begin our discussion with a probabilistic view of form deviations. Using known surfaces, we show how random sampling methods and sample size affect form error estimation. We show how the poor performance of form deviation estimation is tied to the characteristics of the profile. We conclude with a comparison of analysis techniques and a discussion of the role of the metric p in L_p-norm estimation.

2 Statistical Distributions for Surface Profiles and Its Impact on Sampling Results

Definition 1: True Profile: Let the true profile, P, be defined as the actual surface profile of a given workpiece.

Definition 2: True Form Error: Let the true form error, W, be defined as the width of the smallest zone in the form of the nominal geometry that encloses P.

Definition 3: Zone Location Function: Let the location of the form error zone be defined by a function, Z_p^n, corresponding to the nominal geometry defined at the location of the half-width of W. The index p refers to the method used to obtain the zone location and n is the number of sample points. For $p = 0$ and $n = 0$, we use the known zone location and for $p > 0$ we use the L_p − norm estimator.

Definition 4: Measured Form Error: Let the measured form error for n sample points be W_p^n, where p has the same meaning as in the definition of Z_p^n.

Definition 5: Detectability of True Form Error. Detectability, D_p^n, is defined as the ratio of the estimated form error for n sample points to the true form error (i.e., $D_p^n = W_p^n/W$). We will show that the variance of W_p^n is monotonically decreasing with n and thus the mean is enough to define the detectability.

2.1 Distribution of Sample Points. The periodic surface profile shown in Fig. 1 can be represented by the general cosine wave function

$$y(x) = A \cos(bx + c), \tag{2}$$

where, A is the amplitude, b is the frequency and c is the phase angle. Now suppose we perform random sampling of n points (uniformly distributed) along the x axis on the interval $(0, x_0)$, that is, x has a uniform probability density function (pdf) $f(x)$ given by

$$f(x) = \begin{cases} \dfrac{1}{x_0} & 0 \le x \le x_0 \\ 0 & \text{otherwise.} \end{cases}$$

We would like to determine the pdf for the deviation of the sample points from Z_0^0 which is $f(y)$. For one value of y, two possible values of x will match it within one cycle. There are a total of $x_0 b/2\pi$ cycles within $x \in (0, x_0)$. Thus, the inverse function $y^{-1}(x)$ is a real $x_0 b/\pi$-valued function of y, where $x_0 b/\pi$ is forced to be an integer and all of the $x_0 b/\pi$ values have equal probability. Hence,

$$\begin{aligned} f(y) &= \frac{Pr\{y < y(x) \le y + \Delta y\}}{\Delta y} \\ &= \frac{x_0 b}{\pi} \frac{Pr\{x < x(y) \le x + \Delta x\}}{\Delta y} \\ &= \frac{x_0 b}{\pi} \frac{Pr\{x < x(y) \le x + \Delta x\}}{\Delta x} \frac{\Delta x}{\Delta y} \\ &= \frac{x_0 b}{\pi} f(x) \left| \frac{dx}{dy} \right| \\ &= \frac{b/\pi}{|dy/dx|} \quad \text{for} \quad \frac{dy}{dx} \neq 0 \end{aligned}$$

where

$$\left| \frac{dy}{dx} \right| = Ab \sin(bx + c) = Ab\sqrt{1 - \cos^2(bx + c)}$$

$$= b\sqrt{A^2 - y^2}.$$

Thus,

$$f(y) = \begin{cases} \dfrac{1}{\pi\sqrt{A^2 - y^2}} & |y| < A \\ 0 & |y| \ge A. \end{cases} \tag{3}$$

This probability density function, shown in Fig. 2, represents the distribution of possible values for a given sample point from P.

From (3) and Fig. 2 we would like to emphasize the following points.

(1) The tails of the distribution play an important role in evaluating the form errors as we will show in the next section.
(2) The pdf in (3) is not a function of frequency. Thus, detectability using random sampling is the same under different frequencies with this type of periodic profile.
(3) Since the domain of this pdf is the amplitude A, the distribution is the same with different amplitudes of

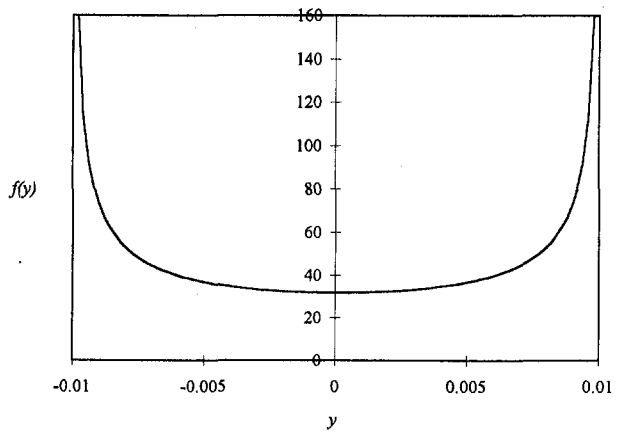

Fig. 2 $f(y) = 1/\pi(0.01^2 - y^2)^{0.5}$ for $|y| < 0.01$; 0 for $|y| \ge 0.01$

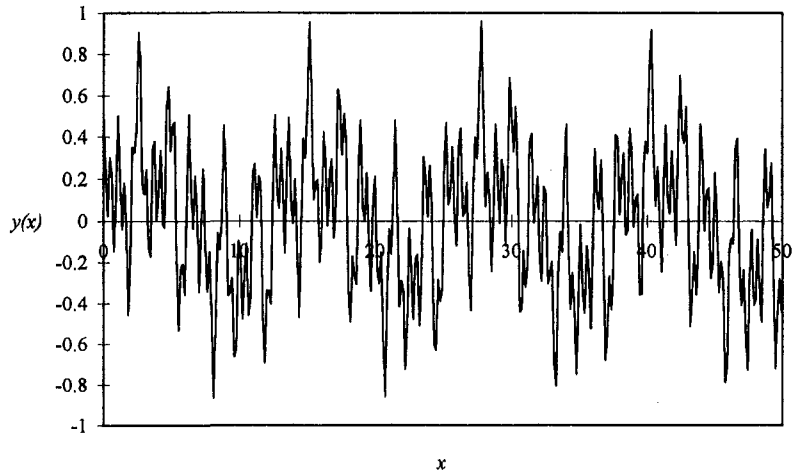

Fig. 3 Profile (4): $y(x) = 0.25$ (sin $3x$ + cos $12x$ + sin $.5x$ + cos $5x$) for $x \in (0, 50)$

$y(x)$. Thus, the detectability using random sampling is the same irrespective of different amplitudes of $y(x)$.

The determination of the form error and the distribution of sample points is more difficult to obtain when we consider more complicated profiles, e.g.,

$$y(x) = 0.25(\sin 3x + \cos 12x + \sin .5x + \cos 5x) \quad (4)$$

for $x \in (0, 50)$, which is shown in Fig. 3. An alternative approach is to estimate Z_0^0 and W_0^0 using Z_∞^n and W_∞^n for large values of n. We can sample a large sequence of points for fixed increments of x and use mini-max optimization to find the zone location. From the zone location, we can create a frequency histogram from the residual values. For example, we sample points at fixed intervals of 0.01 along the x axis ($x \in [0, 50]$). We have 5001 points which are used to approximate the continuous profile (4). Using the L_2 (least squares) estimator, we obtain

$$\hat{Z}_2^{5001} = -0.002868x + 0.071354$$

and using the L_∞ estimator we find a different zone location, namely,

$$\hat{Z}_\infty^{5001} = -0.00001x + 0.047791,$$

for $x \in [0, 50]$. From these estimates (shown in Fig. 4) we observe that the location of the zone is no longer $Z_0^0 = 0$. From the histogram of the sample point deviations (normal distances to Z_∞^{5001}) shown in Fig. 5, we observe that the deviations are clustered about a mean which is not surprising given the profile.

Stout et al. (1990) have provided the height distributions for various machined surfaces, many of which cannot be modeled as a normal distribution. We use the beta distribution, which is not without precedent (He, 1991), to estimate $f(y)$, i.e., the form deviation, for measured profiles. By changing the parameters of the beta distribution, we can control its shape to match that of a specific process (such as those found in our two examples). The probability density function for a generalized beta distribution is given by

$$f(X, \alpha, \beta, a, b) = \frac{1}{(b-a)B(\alpha, \beta)} \left(\frac{X-a}{b-a}\right)^{\alpha-1} \left(1 - \frac{X-a}{b-a}\right)^{\beta-1},$$

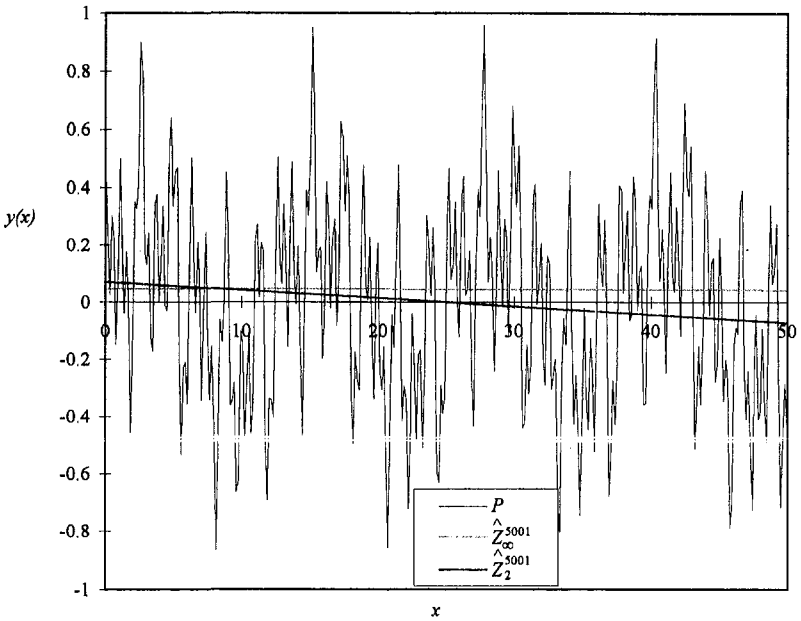

Fig. 4 $\hat{Z}_2^{5001}$ and $\hat{Z}_\infty^{5001}$ for profile (4)

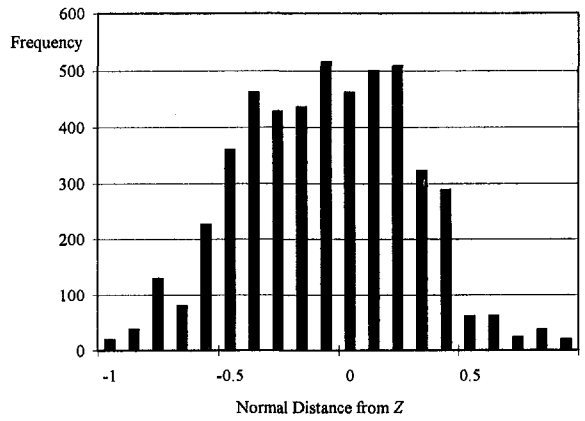

Fig. 5 Sample point distribution function for profile (4)

$$\alpha > 0, \quad \beta > 0, \quad a \le X \le b,$$

where, $B(\alpha, \beta) = \int_0^1 Y^{\alpha-1}(1 - Y)^{\beta-1} dY$, X = random variate (form deviation), a, b = lower and upper limits of the distribution (i.e., l_l and l_u limits of the form error), and α, β = shape exponents. Outside the interval $[a, b]$ the probability density is zero.

We can represent the density function of profile (3) as a beta distribution with $\alpha = \beta = 0.5$, $a = -A$, and $b = A$. The histogram shown in Fig. 5 for profile (4) can be approximated by a beta distribution with $\alpha = 2.683$, $\beta = 2.979$, $a = -0.915$, and $b = 0.914$, using He's algorithm (1991). The estimate of the true form error would be $b - a$ or 1.829.

2.2 Estimated Form Error and Order Statistics. If we take n random samples (following a uniform distribution) from the profile along the x axis, we can treat our points as a set of independent and identically distributed (IID) random variables, $\{Y_1, Y_2, \ldots, Y_n\}$, having a common beta distribution with parameters (α, β). Let the zone location be given as $Z_0^0 = 0$ and let a measured set of sample points, $y_{(1)}, y_{(2)}, \ldots, y_{(n)}$, be sorted in ascending order of magnitude such that

$$y_{(1)} \le y_{(2)} \le \ldots \le y_{(n)}.$$

The samples $y_{(1)}$ and $y_{(n)}$ determine the estimated form error as $w_0^n = y_{(n)} - y_{(1)}$. If we let W_0^n (a random variable) be the difference (the estimated form error) given by $Y_{(n)} - Y_{(1)}$, then the density function of W_0^n (Kendall and Stuart, 1977) for the general case is

$$gW_0^n(w_0^n) = n(n-1) \int_{-\infty}^{\infty} \{F(y_{(1)} + w_0^n) - F(y_{(1)})\}^{n-2} \times f(y_{(1)}) f(y_{(1)}) f(y_{(1)} + w_0^n) dy_{(1)}. \quad (5)$$

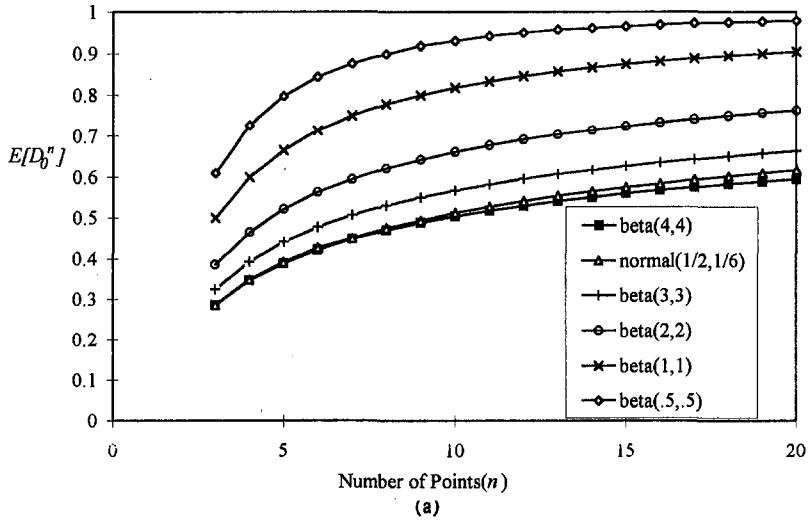

(a)

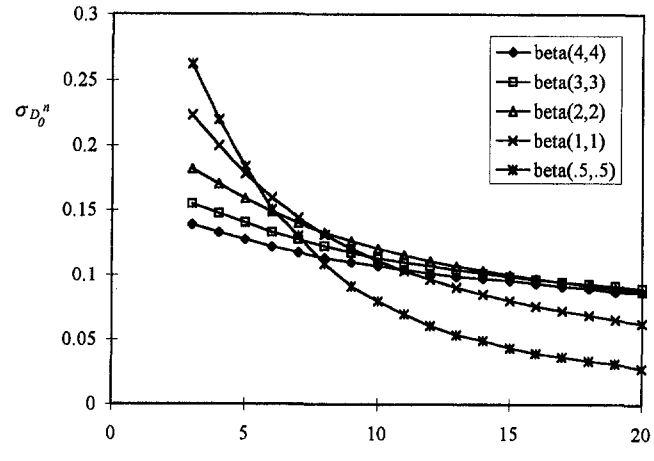

(b)

Fig. 6 (a) Mean (b) standard deviation of range from beta distributions

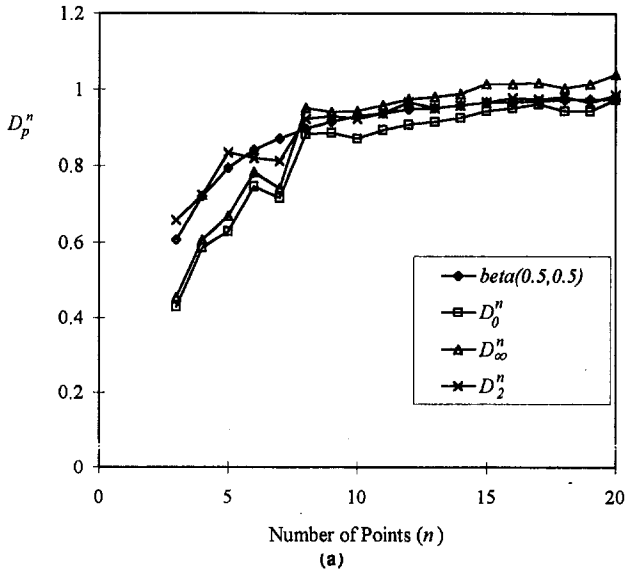

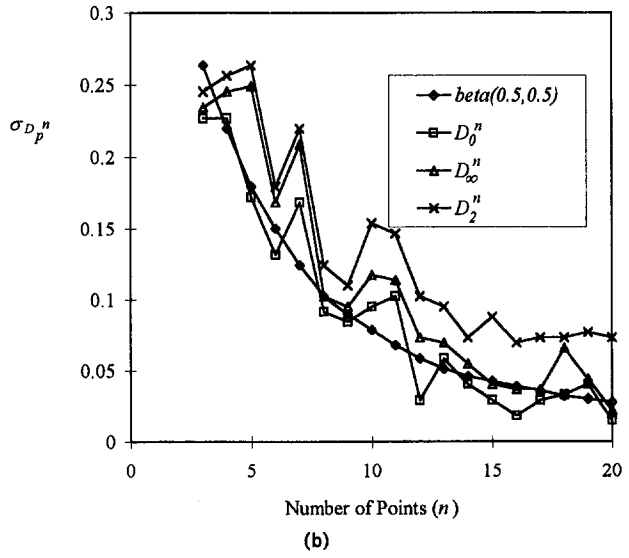

Fig. 7 (a) Mean comparison (b) standard deviation comparison of simulation and theoretical results (Profile S)

Its expected value is

$$E[W_0^n] = \int_{-\infty}^{\infty} \{1 - F(y)^n - [1 - F(y)]^n\} dy \qquad (6)$$

and the mth moment about the mean is given by

$$E[W_0^n - E(W_0^n)]^m = m(m-1) \int_{-\infty}^{\infty} \int_{-\infty}^{y_{(n)}} \{1 - F_n^n - (1 - F_1)^n + (F_n - F_1)^n\} \{W_0^n - E[W_0^n]\}^{m-2} dy_{(1)} dy_{(n)} - (m-1)\{-E[W_0^n]\}^m \quad \text{for } m \geq 2 \qquad (7)$$

From the definition of variance we obtain

$$\sigma_{W_0^n}^2 = E[W_0^n - E[W_0^n]]^2 = 2 \int_{-\infty}^{\infty} \int_{-\infty}^{y_{(n)}} \{1 - F_n^n - (1 - F_1)^n + (F_n - F_1)^n\} dy_{(1)} dy_{(n)} - E[W_0^n]^2. \qquad (8)$$

Using these statistics for the form deviation estimate, we can calculate the detectability with respect to n for given parameters of any distribution. The corresponding expected value and variance for detectability would be given by $E[D_0^n] = E[W_0^n]/W_0^0$ and $\sigma_{D_0^n}^2 = \sigma_{W_0^n}^2/[W_0^0]^2$. Figure 6 shows the results calculated from (6) and (8) for different parameters of beta distributions with $b - a = 1$. From these figures we would like to illustrate the following points.

(1) These figures assume that the zone location, Z_0^0, is known (and therefore independent of n) and the sample points are from IID beta distributions when we perform random sampling.
(2) As sample size increases, detectability increases and the standard deviation decreases.
(3) The detectability for the normal distribution $N(\frac{1}{2}, \frac{1}{6})$, which is close to a unit beta distribution with $\alpha = \beta = 4$ and is the most common form deviation distribution assumption for most researchers, is only 62 percent when we take 20 sample points.
(4) Note that, in practice, typically less than 10 points are used to assess form errors. Therefore, a small sample size has a very high probability of accepting a bad part if the measured zone is the same order of magnitude as the tolerance specification. The scenario is even worse when the form deviation follows a beta distribution

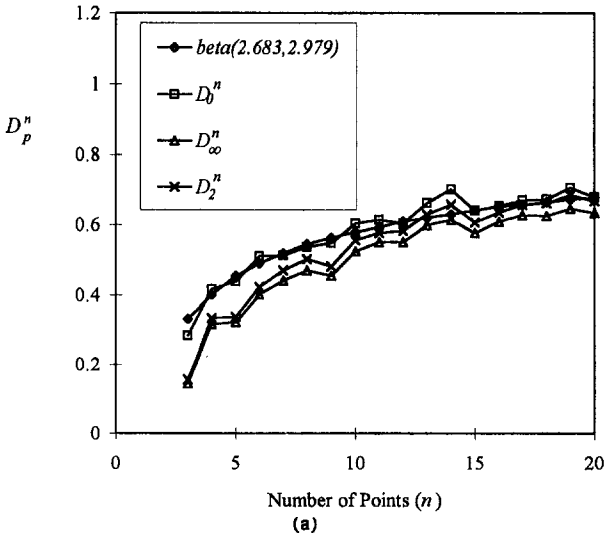

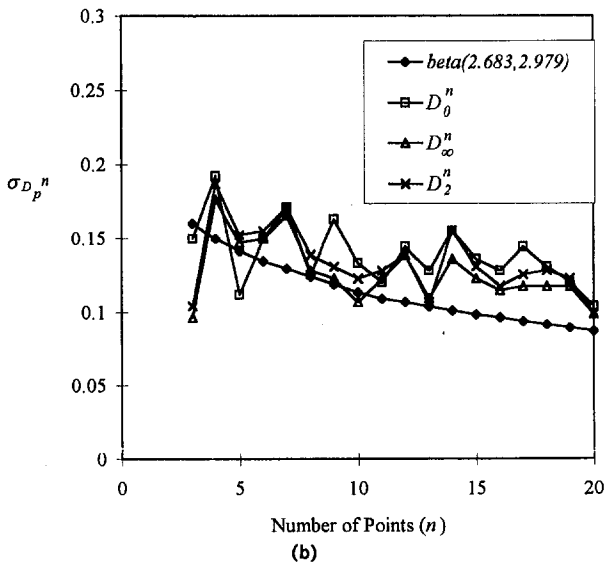

Fig. 8 (a) Mean comparison (b) standard deviation comparison of simulation and theoretical results (Profile B)

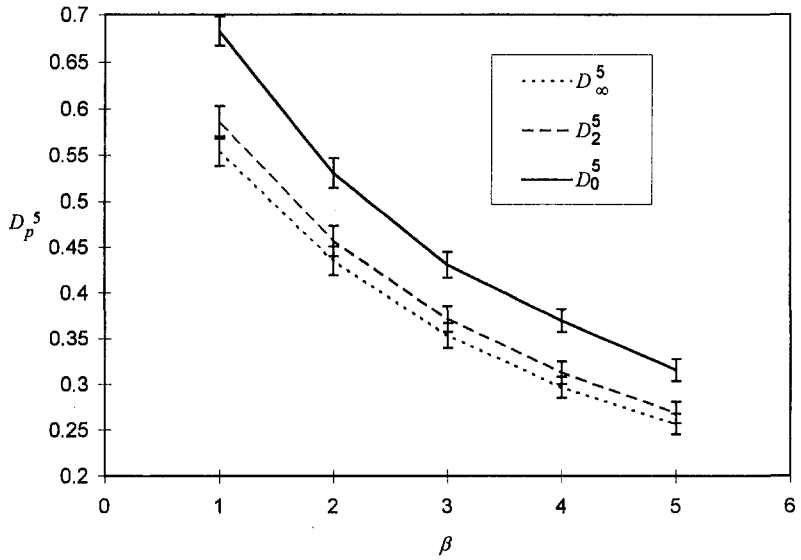

Fig. 9 Detectability for 500 samples, 5 points/sample

with parameters (4, 4) or higher kurtosis. The mean of the estimated form error is only 74 percent of the true value when we take 100 points (82 percent for the normal distribution).

Since the true zone location is unknown to us, the practice is to take an arbitrary number of sample points to estimate Z_p^n and then obtain an estimate of W_p^n. Next, using simulation techniques to take sample points from the two profile examples, we use least squares and mini-max methods to estimate D_p^n for different sets of sample points and compare the results with the theoretical values.

3 Simulated Sampling

3.1 Theoretical versus Measured Form Error. We compare our theoretical results for expected value and variance of the form error from (6) and (8) with form error estimates from simulated inspection sample points by calculating the following.

(1) Theoretical expected value for D_0^n, $E[D_0^n]$
(2) Average detectability using Z_0^n, $\bar{D}_0^n$
(3) Average detectability using Z_2^n, $\bar{D}_2^n$
(4) Average detectability using Z_∞^n, $\bar{D}_\infty^n$

Varying n from 3 to 20, we generate 30 sets of random points from profiles (2) and (4) for each n and then calculate Z_0^n, $\bar{D}_0^n$, Z_2^n. $\bar{D}_2^n$, Z_∞^n, and $\bar{D}_\infty^n$. For profile (2) we use a beta distribution with $a = -0.01$, $b = 0.01$ and $\alpha = \beta = 0.5$. For profile (4), we use a beta distribution with $a = -0.915$, $b = 0.914$, $\alpha = 2.683$, and $\beta = 2.979$. Note that in both cases, $W_0^0 = b - a$.

Figures 7 and 8 show the mean values and standard deviations of D_p^n and the theoretical values calculated by (6) and (8) for profiles (2) and (4), respectively.

Based on these simulation results, we make the following observations:

(1) The difference between the detectability calculated from (6) and the estimates from random sampling for

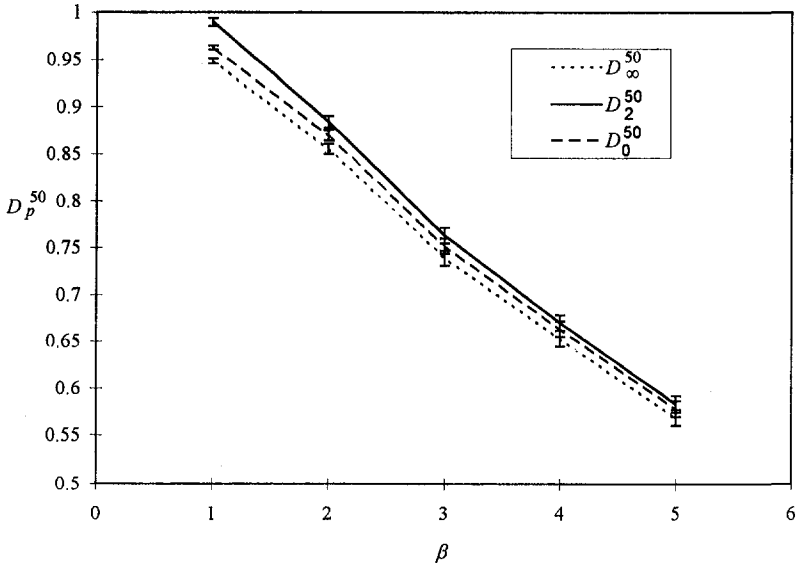

Fig. 10 Detectability for 500 samples, 50 points/sample

both profiles decreases as the sample size increases. We attribute this bias to the estimate of the zone location. As would be expected, small sample sizes exhibit large biases. Later Figs. 9(b) and 10(b) illustrate this point more clearly.

(2) The detectability estimated by the mini-max method is consistently smaller than the $E[D_0^n]$ calculated from (6) for both profiles. This can result in accepting a part which is actually out of tolerance. Therefore, the type II error (the probability of accepting a bad part) is higher when using the mini-max method.

(3) Hopp (1993) suggests that an optimal p value can be found for the parameters of a substitute geometry (i.e., Z_p^n), though the way to make the best choice of p is not clear. For our examples, we did not observe a major difference in the estimates for different values of p. The estimate of detectability, $\bar{D}_0^n$, based on the known Z_0^0 agrees quite well with the mean values calculated from (6).

(4) We observe that even with good estimates of the zone location, the detectability is still quite low (e.g., profile (4)) due to the sampling limitation.

(5) The more complex profile of (4) exhibits much poorer performance for all the estimates.

3.2 Profile Distribution and Form Error. In order to generalize the previous observations, we conducted another simulation study for different beta distributions. We assume $Z_0^0 = 0.5$ as the zone location and the true straightness error as $W_0^0 = 1$. Points on the surface are I.I.D. having a beta distribution with $\alpha = 1$ and β varying from 1 to 5. Five hundred samples are generated for each distribution with 5 and 50 measurement points for each sample. Again we calculate Z_0^n, $\bar{D}_0^n$, Z_2^n, $\bar{D}_2^n$, Z_∞^n, and $\bar{D}_\infty^n$ for each value of n.

Figures 9 and 10 show the 95 percent confidence intervals for detectability for the 500 samples using 5 and 50 measurement points/sample, respectively. We also observed similar behavior for detectability when α was varied.

The detectability calculated from mini-max consistently has the smallest value. The difference is larger for smaller sample sizes which agrees with our previous observation. The normal least-squares method has a higher probability of over-estimating the form error (greater than 1 in this case) especially when $\alpha \leq 1$ and $\beta \leq 1$. In most of the cases, the confidence intervals for $p = 2$ and $p = \infty$ overlap, indicating similar performance for the estimators. Figure 9 exhibits a significant difference between $\bar{D}_0^5$ and the other estimates which shows the effect of using an estimate of the zone location, Z_p^n, on the performance of the detectability estimator.

4 Conclusion

In a discussion at the 1993 International Forum on Dimensional Tolerancing and Metrology, the following points were made.

> In general, we see a point of diminishing returns, after which increasing the number of samples brings no advantage. However, we found that a plot of size vs. number of data points oscillates slightly as it converges, and certain numbers of samples lead to larger errors than adjacent numbers. (For example, 12 points might be worse than 11 or 13 points.) We don't know why this occurs, but it seems to be very repeatable for a given probe and machine. (p. 299)
>
> Our problem, as I see it, is the more points you take, the bigger the value of form error you get. So, we have a curve like this (trending upward as the number of points approached infinity. I don't know of any solid way of estimating, from somewhere here out to infinity, where that curve will go. (p. 301)

Caskey et al. (1992) and Hocken (1993) also reported similar problems. In this paper we have presented a probabilistic viewpoint of the problem by determining the theoretical form error distributions for a wide variety of surfaces profiles under various points of inspection. Our results provide a basis for explaining the empirical evidence of others and indicate that current practices in the evaluation of form are insufficient in dealing with the variety of surface profiles that one encounters due to different manufacturing processes and materials. The surface profile distribution plays a major role in the convergence of form error estimates on the true form error.

Another issue raised in the curve fitting approach is the metric p selection for the fitting objective. From our studies, we have shown that there appears to be no significant difference between $p = 2$ and $p = \infty$ in terms of the detectability. This is due mainly to the standard deviation of the estimates. Sample size and the surface characteristics have the largest effect on detectability.

References

ANSI Y14.5M, 1982, *Dimensioning and Tolerancing, American National Standard, Engineering Drawings and Related Documentation Practices,* The American Society for Mechanical Engineers, New York.

Anderson and Osborne, 1977, "Discrete, Nonlinear Approximation Problems in Polyhedral Norms. A Levenberg-like Algorithm," *Numer. Math.*, 28, pp. 157–170.

Barrodale and Phillips, 1975, "Solution of an Overdetermined System of Linear Equation in the Chebychev Norm," *ACM Trans. on Math. Software*, 1, pp. 264–270, 1975.

Caskey, G., et al., 1991, "Sampling Techniques for Coordinate Measuring Machines," *Proc. of the 1991 NSF Design and Mfg. Sys. Conf.*, January 1991, pp. 779–786.

Caskey, G., et al., 1992, "Sampling Techniques for Coordinate Measuring Machines," *Proc. of the 1992 NSF Design and Mfg. Sys. Conf.*, January 1992, pp. 983–988.

Dhanish, P. B., and Shunmugam, M. S., 1991, "An Algorithm for Form Error Evaluation—Using the Theory of Discrete and Linear Chebyshev Approximation," *Computer Methods in Applied Mechanics and Engineering*, 92, pp. 309–324.

Etesami, F., and Qiao, H., 1989, "Analysis of Two-dimensional Measurement Data for Automated Inspection," *Journal of Manufacturing Systems*, Vol. 9, No. 1, pp. 21–34.

Huang, S. T., Fan, K. C., and Wu, J. H., "New Minimum Zone Method for Evaluating Straightness Errors," *Precision Engineering*, Vol. 15, No. 3, July 1993, pp. 158–164.

Gonin, R., and Money, A. H., 1989, *Nonlinear L_p-norm Estimation*, Marcel Dekker, New York.

He, J. R., 1991, "Estimating the Distributions of Manufactured Dimensions With Beta Probability Density Function," *Int. J. Mach. Tools Manufact.*, Vol. 31, No. 3, pp. 383–396.

Hocken, R. J., Raja, J., and Babu, U., "Sampling Issues in Coordinate Metrology," *Proceedings of the 1993 International Forum on Dimensional Tolerancing and Metrology*, Srinivasan, V. and Voelcker, H. B., eds., CRTD-Vol. 27, pp. 97–111.

Hopp, T. H., 1993, "Computational Metrology," *Proceedings of the 1993 International Forum on Dimensional Tolerancing and Metrology*, Srinivasan, V. and Voelcker, H. B., eds, CRTD-Vol. 27, pp. 207–217.

Kanada, T., and Suzuki, S., "Application of Several Computing Techniques for Minimum Zone Straightness," *Precision Engineering*, Vol. 15, No. 4, Oct. 1993, pp. 274–280.

Kendall, M., and Stuart, A., 1977, *The Advanced Theory of Statistics, Vol. 1, Distribution Theory*, Fourth edition, Charles Griffin & Company Limited, London & High Wycombe.

Menq, C. H., Yau, H. T., and Lai, G. Y., 1990, "Statistical Evaluation of Form Tolerances Using Discrete Measurement Data," *Proceedings of the Symposium on Advances in Integrated Product Design and Manufacturing*, 1990 ASME Winter Annual Meeting, November 25–30, Dallas, TX, pp. 135–150.

Murthy, T. S. R., and Abdin, S. Z., 1980, "Minimum Zone Evaluation of Surfaces," *Int. J. Mach. Tool Des. Res.*, Vol. 20, No. 3, pp. 123–136.

Roy, U., and Zhang, X., 1992, "Establishment of a Pair of Concentric Circles With the Minimum Radial Separation for Assessing Roundness Error," *Computer Aided Design*, Vol. 24, No. 3, pp. 161–168.

Shunmugam, M. S., "On Assessment of Geometric Errors," 1986, *Int. J. Prod. Res.*, Vol. 24, No. 2, pp. 413–425.

Shunmugam, M. S., 1987a, "New Approach for Evaluating Form Errors of Engineering Surfaces," *Computer-Aided Design,* Vol. 19, No. 7, pp. 368–374.

Shunmugam, M. S., 1987b, "Comparison of Linear and Normal Deviations of Forms of Engineering Surfaces," *Precision Engineering,* Vol. 9, No. 2, pp. 96–102.

Shunmugam, M. S., 1990, "Establishing Reference Figures for Form Evaluation of Engineering Surfaces," *Journal of Manufacturing Systems,* Vol. 10, No. 4, pp. 314–321.

Stout, Davis and Sullivan, 1990, *Atlas of Machined Surfaces,* Chapman and Hull.

Traband, M. T., Joshi, S., Wysk, R. A., Cavalier, T. M., 1989, "Evaluation of Straightness and Flatness Tolerances Using the Minimum Zone," *Manufacturing Review,* Vol. 2, No. 3, pp. 189–195.

Woo, T., Liang, R., and Pollock, S., 1993, "Hammersley Sampling for Efficient Surface Coordinate Measurements," *Proc. of the 1993 NSF Design and Mfg. Sys. Conf.,* January 1993, pp. 1489–1495.

Session 10, "The Current State of Affairs," *Proceedings of the 1993 International Forum on Dimensional Tolerancing and Metrology,* Srinivasan, V., and Voelcker, H. B., eds., CRTD-Vol. 27, pp. 297–307.